EROSION BY CONCENTRATED FLOW

ARS 41-179 February 1971

Agricultural Research Service

UNITED STATES DEPARTMENT OF AGRICULTURE

EROSION BY CONCENTRATED FLOW

By Joe C. Willis, research hydraulic engineer,
Soil and Water Conservation Research Division[1]

When water flows on a sloping surface, gravity causes it to seek the lowest levels as determined by the topography of the surface. It finds its way into the crevices between soil aggregates, into furrows and rills, row middles, drainageways, ditches, small streams, and rivers. Each step may be looked upon as progressive concentration of the flow.

As the flow is concentrated, its potential for erosion is also concentrated. If the flow is diffused by a flattening of the slope, its erosive potential may be lessened, and deposition may even occur.

This report pertains to the ability of flowing water to entrain and transport detached material. In other words, such material as soil particles or aggregates has already been detached and is available for transport by the flow. Thus only the transport phase of the erosion model as proposed by Meyer and Wischmeier[2] is considered. This phase was investigated in a laboratory study of the erosion of sand bed material. Laboratory flume tests were designed to investigate the relationships between the erosion rates and flow variables that occurred as the sand bed was degraded by set flow rates and to define the limits of erosion at the points of incipient motion of the bed material.

Experimental Procedure

Data for this investigation were obtained from a laboratory channel 16 feet long by 6 inches wide (fig. 1). An adjustable weir at the downstream end provided an elevation control. A $\frac{1}{8}$-inch slot under the weir passed a small part of the flow along with the bed material and caused the sand bed at the flume exit to assume the

[1]In cooperation with the Mississippi Agricultural Experiment Station and the University of Mississippi.

[2]Meyer, L. D., and Wischmeier, W. H. Mathematical simulation of the process of soil erosion by water. Amer. Soc. Agr. Engin. Trans. 12 (6): 754-758. 1969.

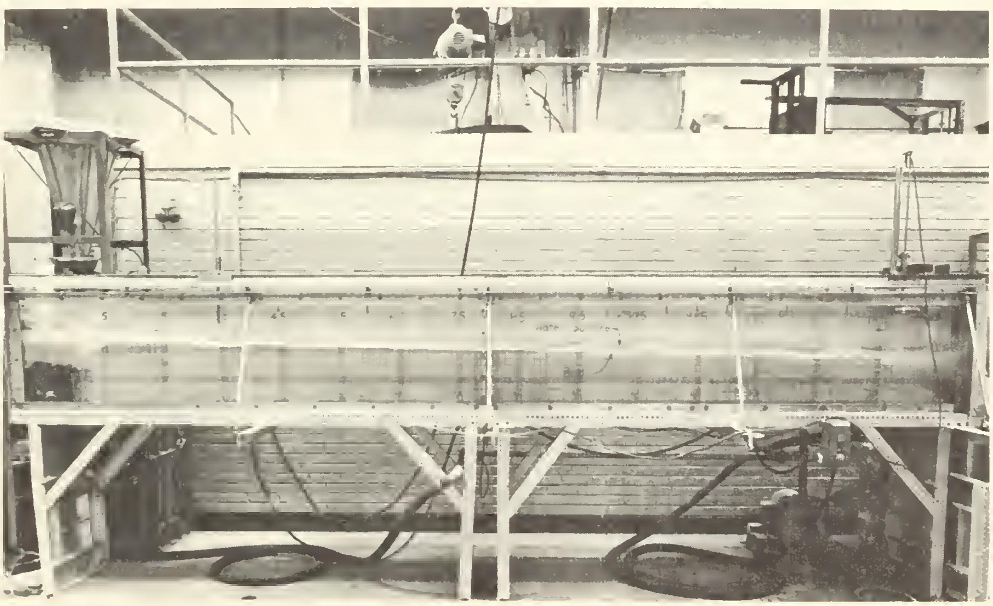

Figure 1.–Erosion test channel with flow near equilibrium for initial sediment feed of sand 2 with q=0.198 c.f.s. per foot.

angle of repose of the material. This reduced the effective length of the erodible sand bed to about 14.5 feet.

The useable discharge range was from 0.09 to 0.30 c.f.s. per foot width of flume. A vibratory sand feeder established an initial capacity transport concentration greater than 20,000 p.p.m. A tank at the end of the channel served to trap the sediment eroded from the sand bed and provided a reservoir for the pumping system.

Three sand bed materials having median diameters of 0.61 (No. 1), 0.31 (No. 2), and 0.40 (No. 3) mm. were used in this investigation. Figure 2 shows the size distribution of the three materials. Sands 1 and 2 were obtained from sand deposits and were rather angular. Sand 3 was from the bed of Cuffawa Creek near Holly Springs, Miss., and its particles were more nearly spherical.

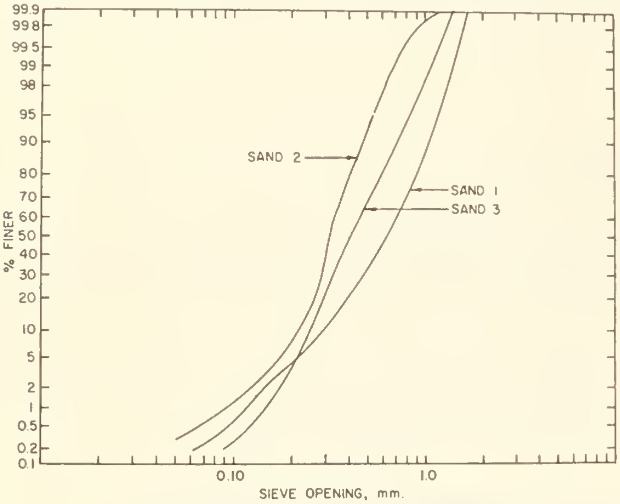

Figure 2.—Sieve analysis of bed materials.

Sands were chosen for this investigation instead of silts or clays because silt- and clay-sized particles probably are seldom detached in sufficient quantities to limit their transport by flow. For a natural soil, sands and aggregates, whose fall velocities are adequate to limit transport, comprise a certain fraction of the soil mass, and a limitation on the transport of this material limits the erosion of the soil mass in general.

Other instrumentation consisted of a point gage to measure elevations along the bed and water surface profiles, a sonar device to record the bed profiles for relatively slow flows with irregular beds, a calibrated elbow meter to determine the flow discharge, and a float and siphon arrangement in the reservoir to provide temperature control by interchanging cool water for warm water.

At the beginning of a typical erosion test, initial equilibrium bed and water surface slopes were established by operating the flume at the selected flow discharge and sand feed rate. The erosion processes were then initiated by stopping the sand feed. The sand bed and water surface profiles were then described by point elevation readings or sonar traverses or both as the initial sloping surface was eroded and degraded by the constant discharge. The tests were repeated for 11 to 13 discharges for each of three bed materials.

At the end of a typical 8-hour erosion test the bed was still being eroded at a low rate (about 0.003 foot per hour). Even after the longest test used (290 hours), sediment motion was still observed over all points on the bed. Yet the erosion processes were approaching some asymptote or final condition that would be reached only after a theoretically infinite time. Incipient motion tests were conducted to estimate this final condition for the hydraulic variables associated with erosion. The main results of this phase of the investigation have been reported.[3]

The procedure for the final conditions tests was to allow the flow and erosion processes to continue (1) for a bed elevation slightly lower than that achieved in the erosion tests, (2) for the base tailgate setting, (3) and for a discharge giving a very low transport rate. The flume was allowed to run under these conditions for at least 24 hours to insure that the bed forms were typical of very low transport conditions. The tailgate was then raised until incipient motion conditions were established.

The criterion used to define "incipient motion" when ripples were present on the bed was that motion was allowed on not more than two nor less than one ripple on a 13-foot length of bed surface. Generally about 15 ripples were present on this length of bed for the two finer bed materials. For the relatively plane bed of the coarser material, no more than one "gust" of sediment motion over a 2-foot length of sand bed was permitted in a 5-second period.

Since the slopes were exceedingly small and the velocities low, subsequent erosion would cause negligible change in the average water surface elevation. Hence, the distance that the water surface was raised in establishing the depth and velocity of flow for incipient sediment motion was taken as an estimate of the distance that the bed would be lowered by erosion after a very long period (theoretically infinite time).

[3]Willis, J. C. Discussion of "sediment transport mechanics: initiation of motion," by Vito A. Vanoni. Amer. Soc. Civ. Engin. Hydraul. Div. Jour. 93 (HYI): 101-107. 1967.

Continuity Equation for Erosion

The definition of erosion in terms of the sediment transport rate becomes the continuity equation

$$\frac{\partial \eta}{\partial t} = -\frac{\nabla . G}{\gamma_s} \qquad (1)$$

where the quantity $\frac{\partial \eta}{\partial t}$ represents the rate of change in the bed elevation η with time t, or the volume rate of erosion or deposition per unit area. The quantity G represents the transport rate of sediment in weight per unit time and unit channel width, and γ_s is the bulk density of the sediment. the quantity $\nabla . G$, or the divergence of G, represents the difference between the inflow and outflow rates of sediment for an increment of area. This expression is generally reduced to the one-dimensional case as $\frac{\partial G}{\partial X}$, where X is distance along a rill, ditch, or river.

The continuity equation is applicable to both erosion and deposition. If the transport rate increases down a rill without a change in the flow discharge, then the rill is being eroded. If the transport rate decreases, then deposition must occur. This is the same concept that Meyer and Wischmeier[4] used in routing the eroded sediment down a slope. The continuity relationship is straightforward *if* we can predict the transport rate and how it changes with distance downslope.

Unfortunately methods of predicting the transport rate for a flow are little more than educated guesses. Several equations have been proposed for relating transport rate to flow variables, but the estimates that they yield for a particular condition may differ by more than 500 percent.[4]

Of course, every set of data contains some error due to imprecision of measurement, but such statistical scatter could hardly account for the observed variations. A distinction between the sediment load and the transport capacity may account for the extreme variability of transport data. Transport capacity may be defined as the rate at which a given flow can transport sediment of a particular particle size through an infinite uniform channel reach having a bed of the same material. Hence, the transport capacity of a given set of hydraulic variables denotes the capacity of the same set of variables and uniform flow. The transport capacity then becomes a unique function of the flow variables and the sediment properties. But for nonuniform flow, the actual sediment load may differ appreciably from the transport capacity.

The actual transport rate may be less than capacity and this is illustrated by figure 3, which shows the bed

[4]See footnote 2.

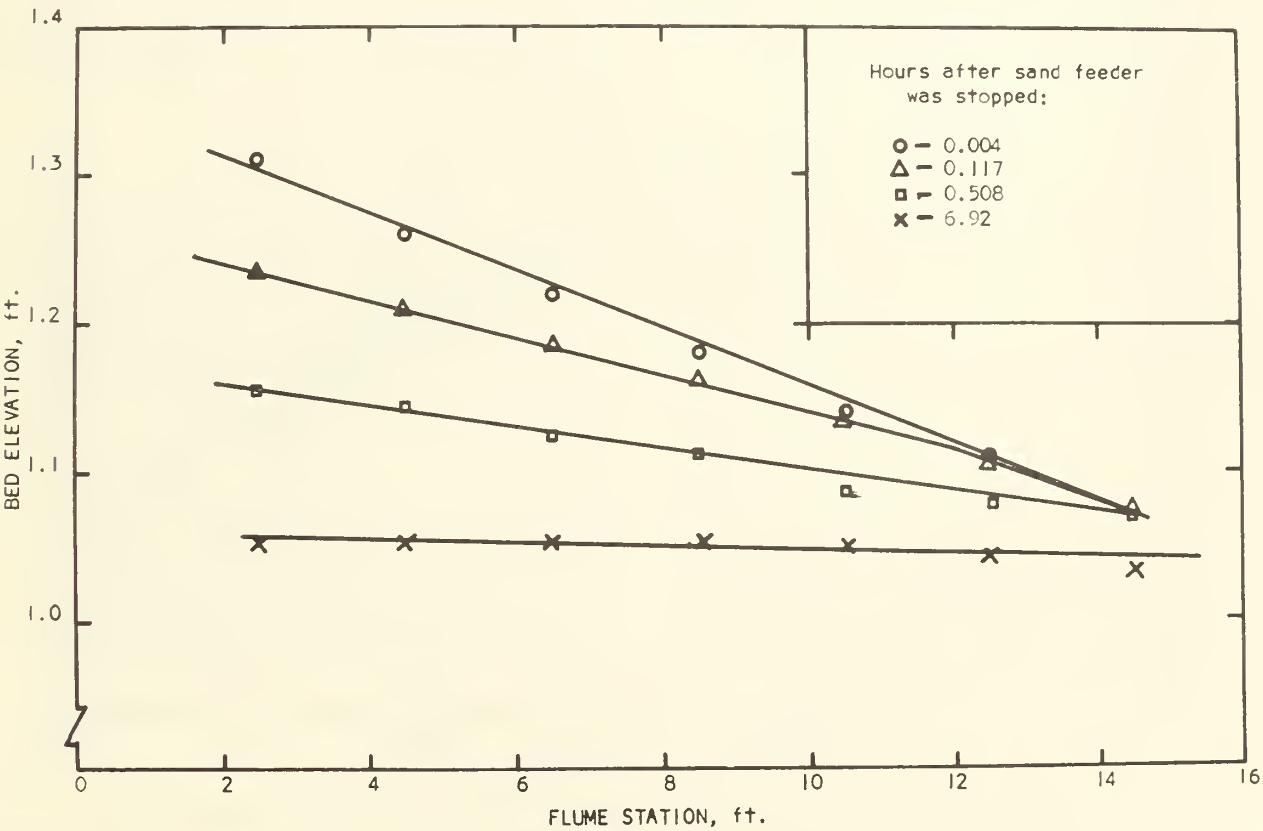

Figure 3.—Typical bed profiles for sand 1 with q=0.126 c.f.s. per foot.

profiles at three times during an 8-hour erosion test. An obvious conclusion that can be drawn from this figure is that the erosion rate was highest near the upstream end of the test channel. In fact, 0.5 hour after erosion had begun in the flume, no erosion had occurred at the downstream end of the sand bed. Until this time the flow had apprently entrained a capacity load by the time it reached the end of the flume. At upstream sections the load was less than capacity, even though the material was sand and hence was detached and available for transport. Thus, for a given set of flow conditions, there is a maximum rate at which flow can entrain a given sediment.

A load in excess of capacity can be transported by steady, nonuniform flow. This is illustrated in figure 4, which shows concentration profiles taken 30, 58, and 82 feet from the entrance to a recirculating flume used in another study.[5] Here the quantity y is the distance from the sand bed and y_t is the flow depth. As the flow proceeded down channel the concentration distribution became more nearly in equilibrium with the flow, and flow variables (velocity and depth) changed, causing a higher transport capacity. At the upstream stations where the depths were relatively deep and velocities low, a higher-than-capacity load was maintained in the upper part of the flow by virtue of the momentum and low fall velocity of the sediment particles, which provide an upper limit on the rate that sediment can be deposited.

When erosion occurs in the field, loads both less than and greater than capacity can occur. Where net erosion is occurring, the sediment load must be less than the transport capacity because of the entrainment rate limitation. Where deposition is observed, a greater-than-capacity load may exist for some distance because of the fall velocity limitation on the deposition rate.

The continuity equation is directly applicable to erosion processes once a capacity load relationship and an entrainment function that describes load variations are developed. Until reliable load and entrainment functions are available, the researcher must resort to experimentation to generate erosion predictions. This is essentially the approach followed in this investigation.

[5] Willis, J. C. An error function description of the vertical suspended sediment distribution. Water Resources Res. 5 (6): 1322-1329. 1969.

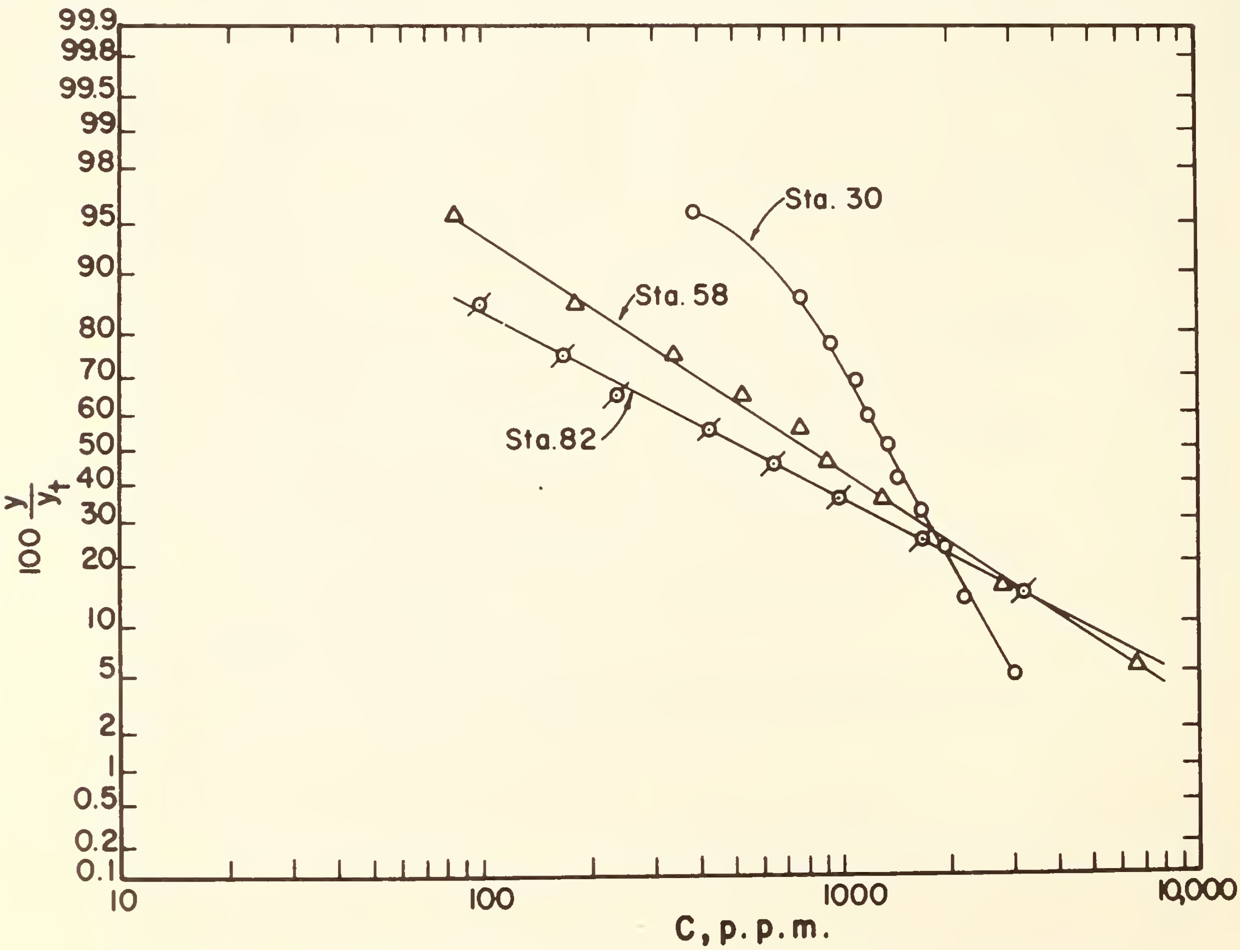

Figure 4.—Concentration profiles taken at stations 30, 58, and 82 feet from the entrance to a recirculating flume.

The short test channel, bed irregularities, and small rates of change in bed elevation resulted in data that were only reliable enough to determine the average erosion rates for the test channel. However, figure 3 does permit a rough interpretation of how the erosion rates varied with distance down the channel and suggests the form that an entrainment function for erosion by concentrated flow might assume. Since the actively eroding sections of the bed profiles can be approximated by straight lines, the erosion rate varied nearly linearly down the channel. If the distance downstream X_c where a capacity load would be entrained is introduced, this linear relationship becomes

$$\frac{\partial \eta}{\partial t} = \left.\frac{\partial \eta}{\partial t}\right|_{X=0} \left(1 - \frac{X}{X_c}\right) \tag{2}$$

At $X = X_c$, the transport rate is the capacity rate G_c, and the average erosion rate upstream from this point is $\frac{G_c}{\gamma_s X_c}$. From equation (2) this average erosion rate can also be expressed as $\frac{1}{2}\left.\frac{\partial \eta}{\partial t}\right|_{X=0}$ so that by substitution equation (2) becomes

$$\frac{\partial \eta}{\partial t} = \frac{2G_c}{\gamma_s X_c}\left(1 - \frac{X}{X_c}\right) = \frac{1}{\gamma_s}\frac{\partial G}{\partial X} \tag{3}$$

Integrating equation (3) for the transport rate at points along the channel gives

$$\frac{G}{G_c} = \frac{X}{X_c}\left(2 - \frac{X}{X_c}\right) \tag{4}$$

Thus the erosion rate depends not only on the transport capacity but also on the relative excess of the capacity over the transport rate. Equations (3) and (4) also illustrate the importance of channel length in interpreting erosion data. Longer channels will yield lower average erosion rates, other things being equal. Only erosion rates based on the capacity entrainment distance X_c will be unique for the same flow variables in channels of different length.

In many erosion problems the degradation of the surface may be negligible, that is, the overall soil surface slope does not change significantly for the period of consideration. For such cases, G_c and X_c may be approximately constant for given flow rates. However, for the flume erosion tests, the slope and flow variables changed with time and the transport capacity as defined by these variables must have changed also. In a long reach, the initial degradation at the upstream end would impart observable flow nonuniformities, and transport capacity G_c and the capacity entrainment distance X_c would vary with both time and distance along the reach. Thus equations 2 through 4 must be considered as approximate relationships based on the average G_c and X_c quantities and the average flow variables for the short test channel. Although these values could not be reliably determined from the flume data, they must be functions of the flow variables and the sediment and, therefore, the resulting average erosion rates must also depend on the flow variables and sediment as well as the length of the test reach.

The flow variables themselves are generated by the flow quantity, the slope of the soil surface or waterway, and the roughness of the soil surface. Flow variables such as velocity and depth could be specified but would be somewhat difficult to determine and would be less convenient to apply to actual erosion problems.

Thus the basic set of independent variables upon which the average erosion rate $\overline{\frac{\partial \eta}{\partial t}}$ or other variables may be considered to depend are unit width flow discharge q, slope S, channel length L, soil properties, and fluid properties, for the assumption that width effects are negligible. In functional form (f) this relation becomes

$$\overline{\frac{\partial \eta}{\partial t}} = f\,(q, S, L, \gamma_s, D, s.f., \sigma, \gamma_\omega, \nu, g) \tag{5}$$

where g is the gravitation constant: the bulk density γ_s, median diameter D, shape factor s.f., and geometric standard deviation σ of the size distribution are taken to characterize the sand bed material, and the unit weight γ_ω and kinematic viscosity ν of the water specify the fluid properties.

For the purposes of this investigation, since L, γ_s, γ_ω, ν, and g were constant or essentially constant, the functional relationship reduces to

$$\overline{\frac{\partial \eta}{\partial t}} = f\,(q, S, D) \tag{6}$$

where D should be considered as a code designation of the sediment material encompassing the other sediment properties as well, rather than indicative of only diameter dependency.

The average erosion rate $\overline{\frac{\partial \eta}{\partial t}}$ is defined as the average rate of lowering of the channel bed, which is equivalent to the volumetric erosion rate per unit of bed area; however, an incremented approximation as $\frac{\overline{\Delta \eta}}{\Delta t}$ resulted in considerable scatter, since the elevation changes in short time intervals were small. Fortunately the average bed elevation was found to describe hyperbolic functions with time of the form

$$\bar{\eta} - \eta_o = \kappa \, (t - t_o)^{-m} \tag{7}$$

where η_o is the elevation of the channel bed at which incipient motion of the sediment would exist and m, κ, and t_o are parameters of the function. Values of η_o were determined from the final conditions tests as a function of flow discharge as shown in figure 5. Since only two parameters can be determined from a least squares analysis of the data, a trial-and-error procedure was necessary to evaluate the other parameters.

Several curves of the form

$$\eta_1 = \kappa_1 T_1^{-m_1} \tag{8}$$

encompassing the shapes of the 8-hour erosion sequences were established on tracing paper. Superimposing these tracings over the data curves permitted the parameter m_1 to be estimated as well as shifts in $\bar{\eta}$ and t to define the sequence of η_1 and T_1 values. Initial estimates of the erosion rates were then made by differentiating equation (8).

$$\overline{\frac{\partial \eta}{\partial t}} = \frac{\partial \eta_1}{\partial t_1} = -\frac{m_1 \eta_1}{T_1} \tag{9}$$

Differentiating equation (7) gives a similar expression

$$\overline{\frac{\partial \eta}{\partial t}} = -\frac{m(\bar{\eta} - \eta_o)}{t - t_o} = -\frac{m\,(\bar{\eta} - \eta_o)}{T_1 - \Delta t} \tag{10}$$

where the quantity $t - t_o$ is denoted as a change Δt from T_1.

Equating these two expressions for $\overline{\frac{\partial \eta}{\partial t}}$ and grouping terms gives

$$T_1 \frac{\frac{\partial \eta_1}{\partial T_1}}{\bar{\eta} - \eta_o} - \Delta t \frac{\frac{\partial \eta_1}{\partial T_1}}{\bar{\eta} - \eta_o} + m = 0 \tag{11a}$$

or

$$Y_1 - \Delta t X_1 + m = 0 \tag{11b}$$

Thus equations (11) define a straight line in the variables Y_1 and X_1 so that the slope $-\Delta t$ and intercept m could be evaluated by a least squares analysis of the data. Revised erosion rate estimates were then computed for the new m and $t - t_o$ values and the least squares analysis was repeated until no additional adjustments in m or $t - t_o$ were indicated. Usually no significant change was observed after the second trial. The average erosion rate associated with each set of water surface and bed profiles was then determined from equation (10) and for the final t_o and m values.

The slope variable constitutes the only other variable associated with equation (6) that is not self-explanatory. In a relatively long channel, the energy grade line, water surface, and bed will be essentially parallel and hence will define only one slope value. For a short channel like the one used in this erosion investigation, the bed and water surface slopes may be different. For nonuniform conditions, the elevation of the energy grade line H may be expressed as

$$H = \frac{q^2}{2gy_t^2} + Z \tag{12}$$

where y_t is the average flow depth and Z is the water surface elevation. The energy slope, which is the most consistent slope estimate for nonuniform flow, is then defined as $-\frac{\partial H}{\partial X}$ or

$$S = -\frac{\partial H}{\partial X} = \frac{q^2}{gy_t^3}\frac{\partial y_t}{\partial X} - \frac{\partial Z}{\partial X} \tag{13}$$

The quantity $-\frac{\partial Z}{\partial X}$ defines the water surface slope S_w, and the depth gradient $\frac{\partial y_t}{\partial X}$ is simply the difference in the bed slope S_b and water surface slope. Equation (13) can then be expressed as

$$S = S_w - \frac{q^2}{gy_t^3}(S_w - S_b) \tag{14}$$

The bed and water surface slopes were then determined by a least-squares fit of straight lines to the profile data and the energy slope was then calculated by equation (14).

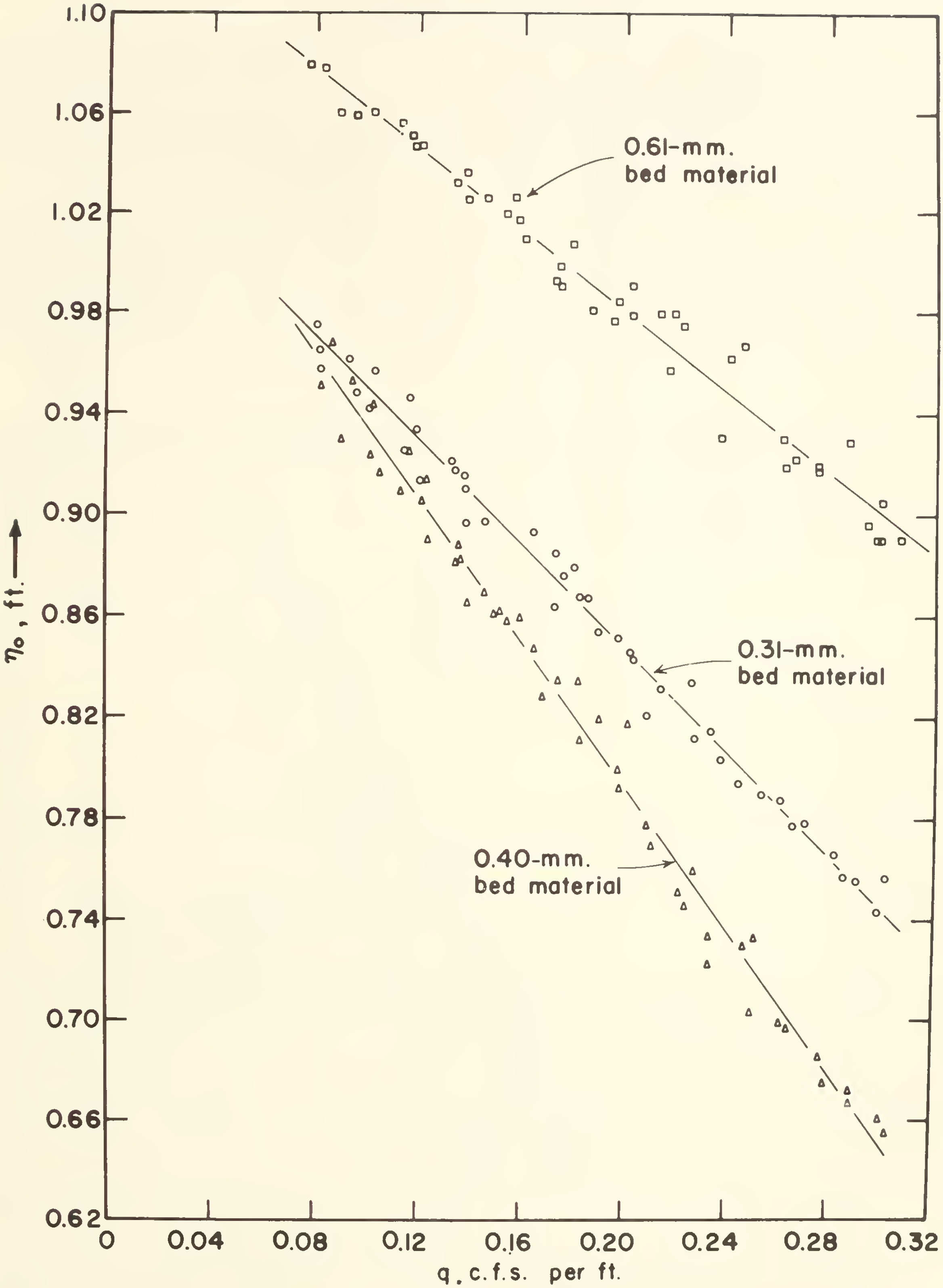

Figure 5.—Limiting elevations for degrading beds.

The empirical relationships as indicated by equation (6) are shown in figures 6, 7, and 8 for the data from three of the erosion tests with each bed material. Tests with an intermediate discharge are included along with two extreme discharge tests to serve as examples. A summary of the data from the erosion tests is included in the appendix.

The data curves for each discharge define unique relationships between average erosion rate and energy slope with only a small amount of scatter. The variation of erosion rate with slope and discharge is clearly illustrated by these relationships between the basic variables. The effects of the different sediments is not so well defined and seems to be unimportant except for small slope values. The erosion rate for the finer material (0.31 mm.) seems to be lower than that for the other sands for similar discharges and erosion rates of less than about 0.04 foot per hour.

The apparent low erodibility of the 0.31-mm. sand is supported by the final elevation results in figure 5. Incipient motion conditions were established at higher bed elevations for this material than for the 0.40-mm. material. Particle shape may account for part of this unexpected result. The grains of the 0.31-mm. material

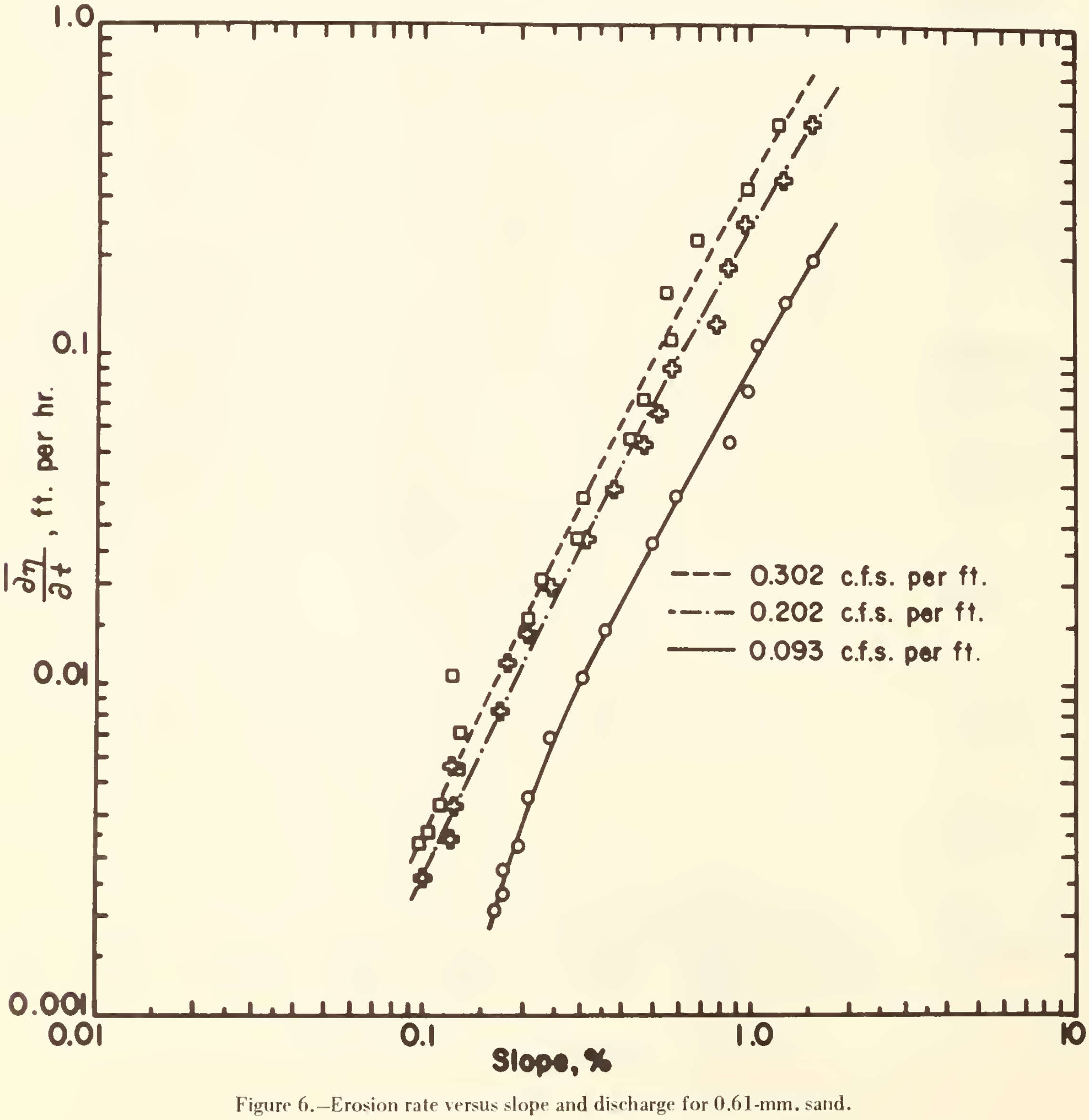

Figure 6.—Erosion rate versus slope and discharge for 0.61-mm. sand.

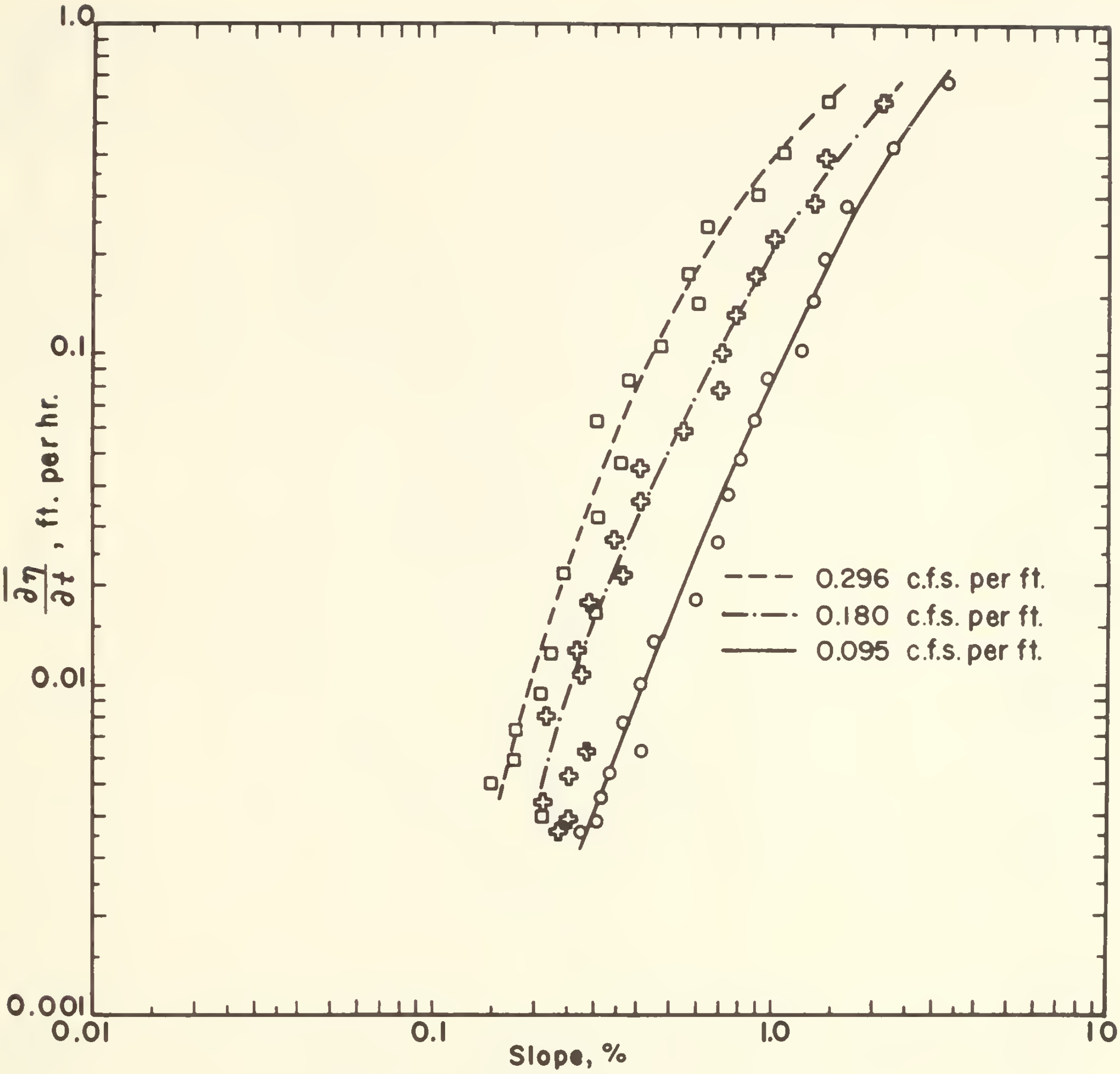

Figure 7.–Erosion rate versus slope and discharge for 0.31-mm. sand.

were quite angular. Also, the high-velocity gradients near the bed would result in finer particles being less exposed than coarser ones to the forces of the flow.

Although relationships like those in figures 6, 7, and 8 are not dimensionally homogeneous, they are probably in the most convenient form for application to the erosion process in the field. Discharge could be determined from the excess rainfall rate, and the surface slope should closely approximate the energy slope. Different curves for different soils and different slope lengths would be required, but our present knowledge of a soil's susceptibility to erosion and of the entrainment process is not adequate to alleviate this requirement.

Similitude principles offer a means to make experimental relationships dimensionally homogeneous and independent of the scale of the system. In connection with transport capacity investigations at the U.S. Department of Agriculture Sedimentation Laboratory, Oxford, Miss., the similitude concepts of fluid mechanics have been successfully applied in unifying capacity relationships for the available flume transport data.[6] The average concentration of sediment at capacity was found to depend on the Froude number $\frac{q}{\sqrt{gy_t^3}}$ and a grain diameter similitude number $\frac{Dg^{\frac{1}{3}}}{\nu^{\frac{2}{3}}}$. Similitude theory suggests

[6]Willis, J. C., and Coleman, N. L. Unification of data on sediment transport in flumes by similitude principles. Water Resources Res. 5 (6): 1330-1336. 1969.

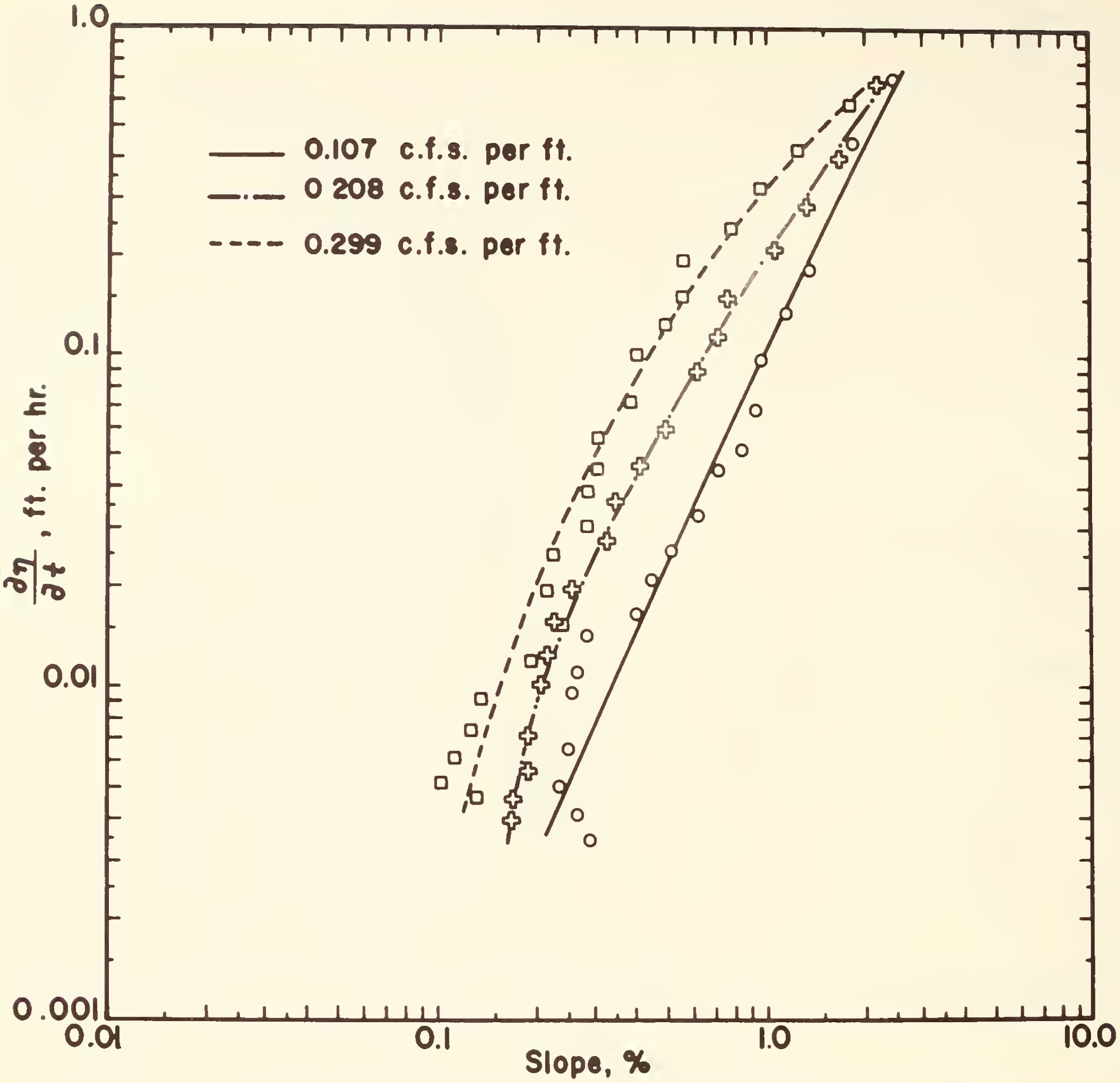

Figure 8.—Erosion rate versus slope and discharge for 0.40-mm. sand.

that the Reynolds number $\frac{q}{\nu}$ may also be important, but for the high Reynolds numbers of the transport capacity tests, the Reynolds number effect was negligible.

The use of these similitude numbers in expressing the results of the erosion tests involves the use of the depth y_t in lieu of the slope in equations (5) and (6). Although the depth may be somewhat difficult to determine for actual erosion problems, the substitution is legitimate since the variables are interdependent.

The concentration of sediment in the flow leaving the eroding channel was determined by

$$C = \overline{\frac{\partial \eta}{\partial t}}\, \gamma_s \frac{L}{q\gamma_\omega} \qquad (15)$$

where values of 100 pounds per cubic foot for γ_s and 14.5 feet for L were used. Here C represents the weight of sediment in a unit weight of water.

Initial efforts to correlate sediment concentration and the Froude number for the erosion tests revealed different curves for different Reynolds numbers. Dual Reynolds and Froude dependency can often be difficult to handle for different scaled systems. Fortunately the curves of C versus Froude number were nearly parallel on exponential paper, with the curves for different Reynolds numbers being separated throughout the range of the data by a nearly constant shift in the Froude number. If this trend should continue for all concentrations down to zero, then physical significance in terms

of a critical Froude number for sediment motion could be assigned to the separation of the data curves.

From the depth y_c and discharge q measurements for incipient motion tests, critical Froude numbers for sediment motion were computed by

$$F_c = q\sqrt{gy_c^3} \tag{16}$$

Figure 9 shows the results as critical Froude number F_c versus Reynolds number. Again the 0.31-mm. material can be seen to be less susceptible to erosion for low flows than the 0.40-mm. material. For each of the bed materials, the critical Froude number decreases with increasing Reynolds number.

Figures 10, 11, and 12 show the erosion concentration as a function of excess Froude number over critical. The critical Froude number shifts collapse the curves for each bed material into one. The three curves deviate from each other for certain ranges of $F - F_c$ values; therefore, the concept of a critical Froude number for sediment motion does not adequately account for the effects of sediment properties. Although the 0.40-mm. material was eroded more easily by the low Froude numbers of the incipient motion tests, the concentrations of this material that were entrained during the erosion tests were lower than the concentrations of the other two materials for most $F - F_c$ values.

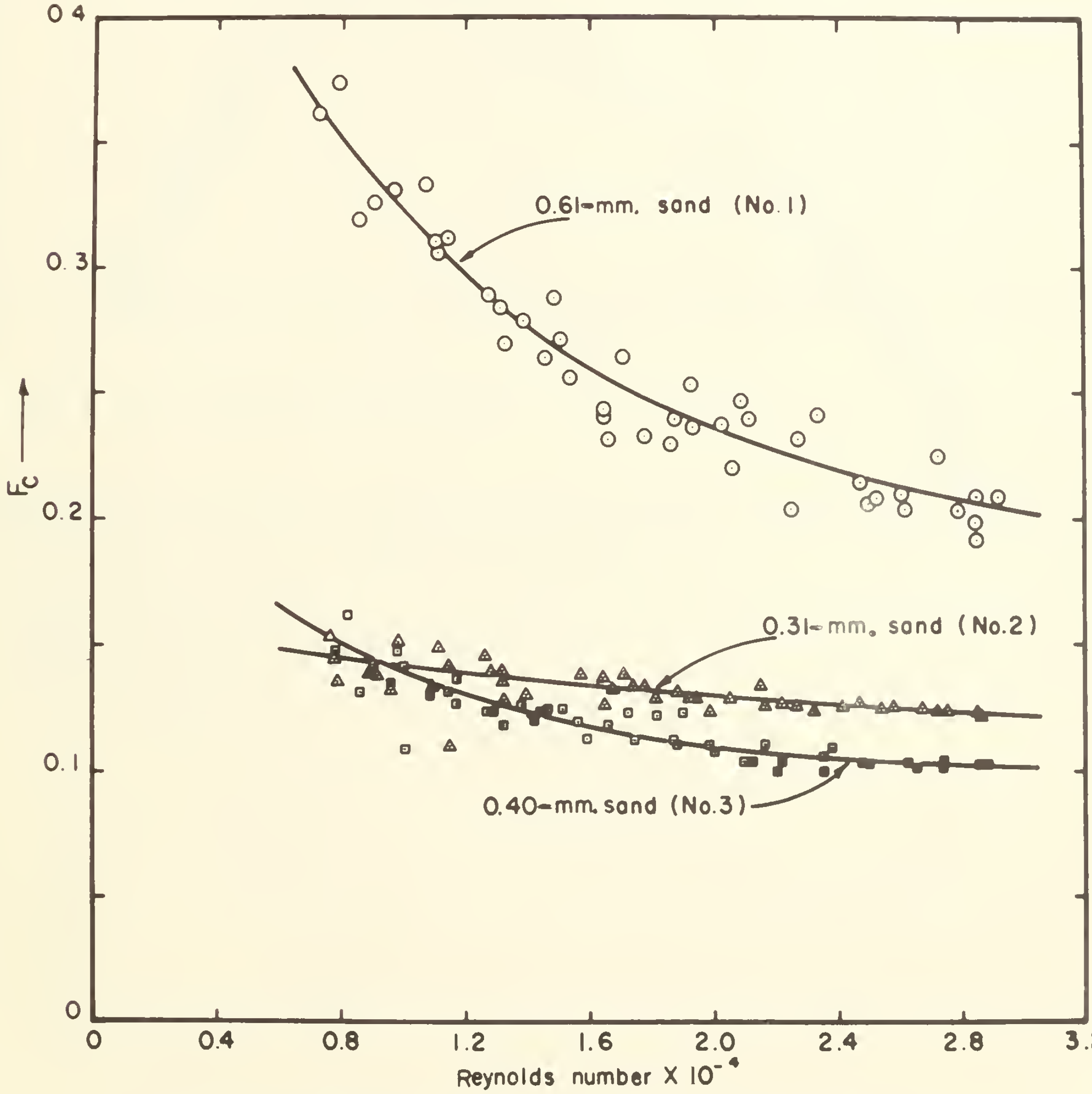

Figure 9.—Critical Froude number for sediment motion from incipient motion tests.

Although the graphical relationships of figures 10, 11, and 12 are expressed in terms of valid similitude numbers, the results cannot be viewed as completely general. If a capacity load were entrained before the end of the channel, then the results would be general for flow conditions meeting this criterion. If a valid entrainment function were available, then results from an experiment such as this one for a limited length of erodible surface could be expressed in terms of other lengths and the capacity transport condition as well.

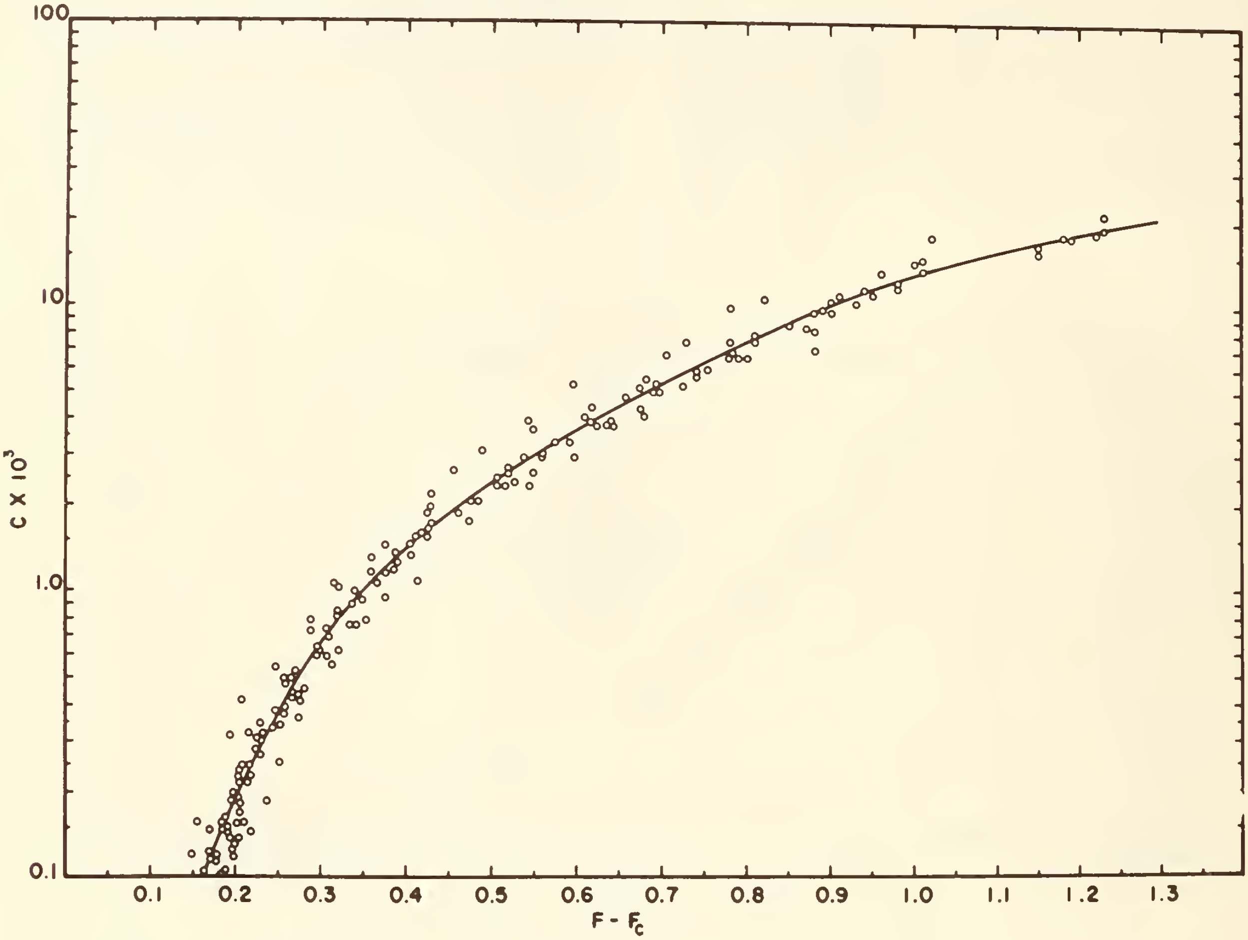

Figure 10.—Concentration of 0.61-mm. sand eroded from test channel as a function of excess Froude number over critical.

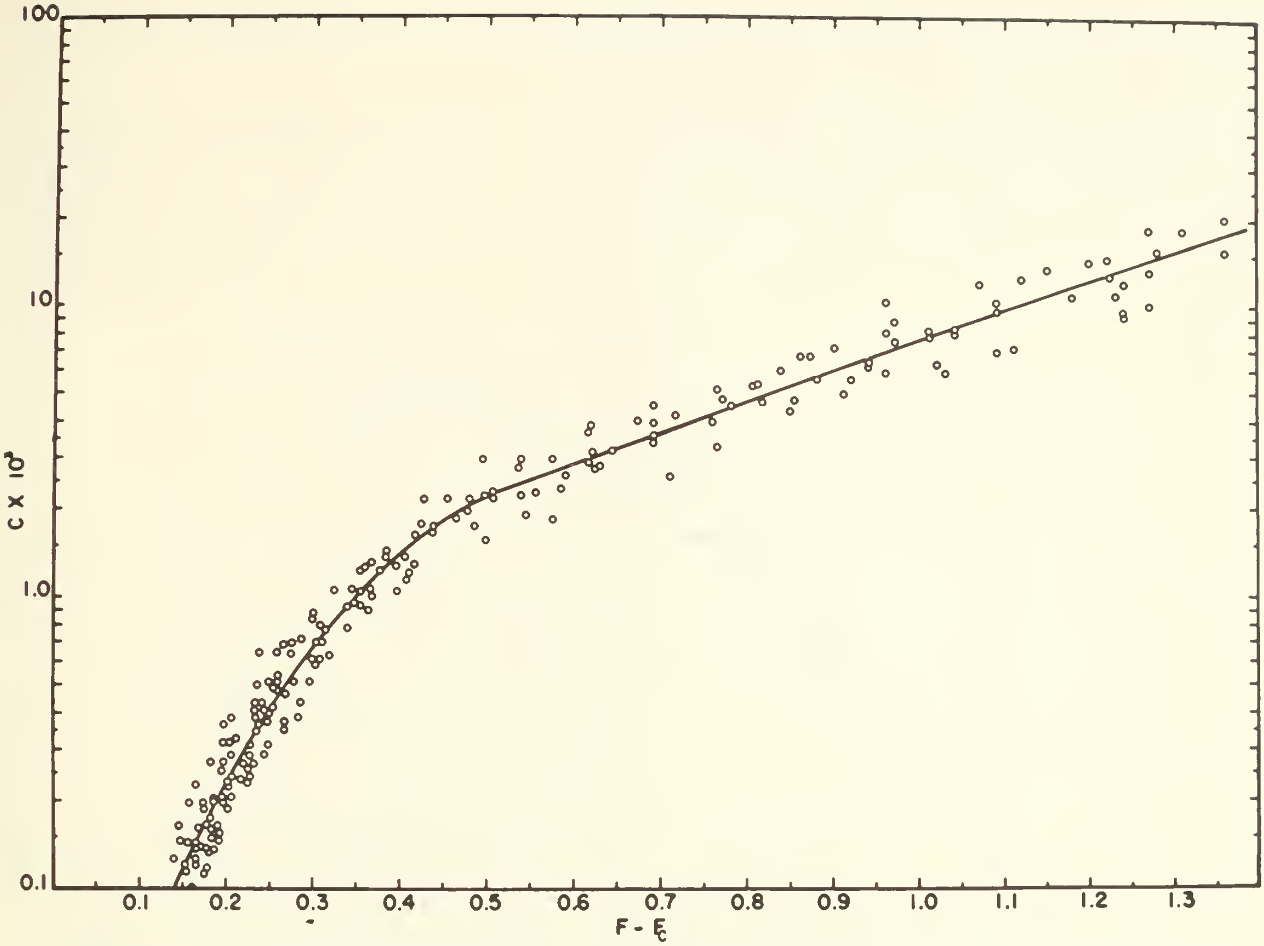

Figure 11.—Concentration of 0.31-mm. sand eroded from test channel as a function of excess Froude number over critical.

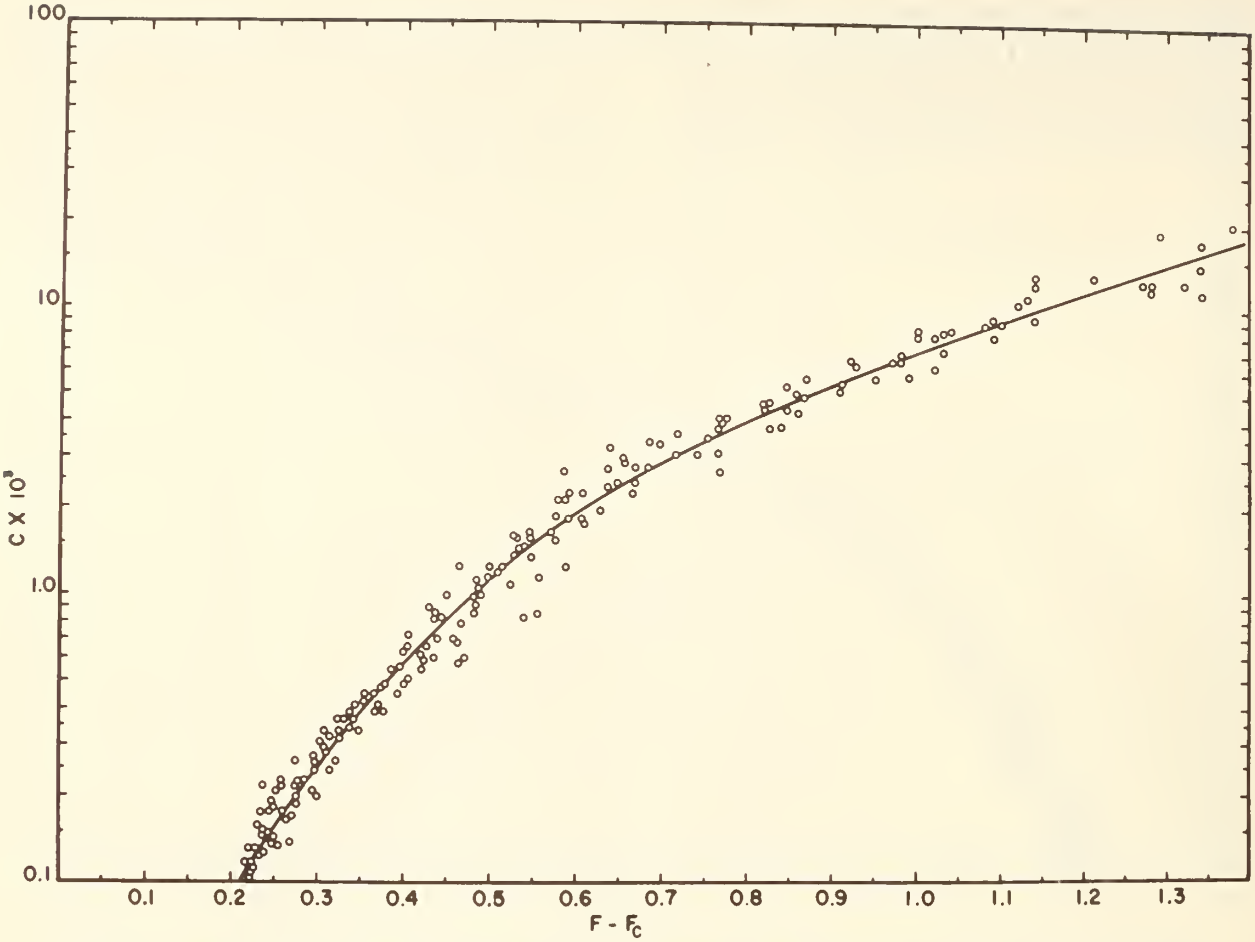

Figure 12.—Concentration of 0.40-mm. sand eroded from test channel as a function of excess Froude number over critical.

Summary

Erosion tests were conducted in a laboratory channel to investigate the relationships between the hydraulic parameters of shallow flows and the erosion rates of sand bed material. The results were expressed in terms of the basic controlling variables of the flow system as well as dimensionless quantities. Although the basic variable relationships may be most convenient for application to similar eroding systems, the data analysis based on transport and flow similitude with addition of the concept of a critical Froude number for sediment motion presented single curves for each bed material.

Appendix

List of Symbols

- C – Sediment concentration, weight of sediment in unit weight of water.
- D – Median diameter of sediment particles.
- F – Froude number.
- F_c – Critical Froude number for sediment motion.
- f – Functional notation.
- G – Sediment transport rate per unit of channel width, pounds per second per foot.
- G_c – Sediment transport capacity, pounds per second per foot.
- g – Gravitation acceleration, feet per second squared.
- H – Elevation of energy grade line, feet.
- L – Length of test reach downstream of point of zero sediment transport rate, feet.
- m – Exponent of erosion time variation function.
- m_1 – Initial estimate of m in trial computations.
- q – Flow discharge per unit of channel width, cubic feet per second per foot.
- S – Slope of energy grade line.
- S_b – Average slope of channel bed.
- S_w – Average slope of water surface.
- s.f. – Shape parameter of sediment grains.
- T_1 – Initial trial estimate of quantity $(t - t_o)$, hours.
- t – Time after initial sediment feed was stopped, hours.
- t_o – Time asymptote of erosion transition function, hours.
- X – Distance down channel, feet.
- X_c – Distance down channel required for given set of flow variables to entrain a capacity sediment load, feet.
- X_1 – Variable denoting quantity $\dfrac{\frac{\partial \eta_1}{\partial T_1}}{\eta - \eta_0}$.
- Y_1 – Variable denoting quantity $T_1 \dfrac{\frac{\partial \eta_1}{\partial T_1}}{\eta - \eta_0}$.
- y – Vertical distance from channel bed, feet.
- y_c – Critical flow depth for sediment motion, feet.
- y_1 – Flow depth, feet.
- Z – Water surface elevation, feet.
- γ_s – Bulk unit weight of bed material, pounds per cubic foot.
- γ_ω – Unit weight of water, pounds per cubic foot.
- Δ – Denotes incremented variable.
- η – Bed elevation, feet.
- η_o – Average bed elevation that should exist in test channel after all erosion stopped, feet.
- $\bar{\eta}$ – Average bed elevation of test channel, feet.
- η_1 – Initial trial estimate of quantity $(\eta - \eta_o)$, feet.
- κ – Coefficient in erosion time transition function.
- κ_1 – Initial estimate of κ.
- ν – Kinematic viscosity of water, square foot per second.
- σ – Geometric standard deviation of the particle size distribution.
- ∇ – Laplacian operator.

Table 1.—*Summary of test data*

Test	q c.f.s. per ft.	Temperature °F.	q/v 0.10^{-F}	m	η_0 Ft.	F_c
1- 1	0.0926	77	0.961	0.421	1.068	0.327
1- 2	.1256	75.5	1.28	.426	1.040	.288
1- 3	.1462	76	1.50	.359	1.021	.267
1- 5	.1826	74	1.82	.270	.993	.246
1- 6	.2016	73.5	2.00	.245	.978	.236
1- 7	.2206	70	2.09	.229	.963	.232
1- 8	.2276	73	2.24	.233	.959	.225
1- 9	.2690	74	2.68	.204	.927	.211
1-10	.3026	73.5	3.00	.175	.901	.203
1-11	.2736	72	2.66	.203	.922	.210
1-13	.1724	72	1.68	.300	1.001	.254
2- 1	.0950	69	1.12	.199	.955	.140
2- 2	.1350	68.5	1.25	.184	.914	.138
2- 3	.2008	65.5	1.79	.156	.847	.131
2- 4	.2600	68	2.40	.146	.786	.126
2- 5	.1980	70	1.88	.163	.848	.130
2- 6	.2280	69.5	2.15	.161	.818	.128
2- 7	.1800	63.5	1.56	.168	.868	.134
2- 8	.2130	65.5	1.90	.159	.834	.130
2- 9	.2960	65	2.62	.132	.748	.125
2-10	.1118	70	1.06	.182	.938	.140
2-11	.2820	70	2.67	.136	.765	.124
3- 2	.1074	70	1.02	.186	.925	.138
3- 3	.1290	70	1.22	.179	.894	.130
3- 4	.1500	70	1.42	.154	.865	.122
3- 5	.1702	70	1.61	.136	.836	.117
3- 6	.1940	70	1.84	.131	.802	.112
3- 7	.2080	70	1.97	.123	.782	.110
3- 8	.2302	70	2.18	.122	.750	.107
3- 9	.2500	70	2.37	.111	.722	.105
3-10	.2738	70	2.59	.106	.687	.103
3-11	.2994	70	2.83	.100	.651	.102